N- and *P*-type dopant profiles in distributed Bragg reflector structures and their effect on resistance

R. F. Kopf, E. F. Schubert, S. W. Downey, and A. B. Emerson
AT&T Bell Laboratories, Murray Hill, New Jersey 07974

(Received 18 March 1992; accepted for publication 30 July 1992)

We report the *n*- and *p*-type dopant profiles obtained in AlAs/GaAs structures. When structures were doped with Si or C, targeted dopant profiles were achieved. However, when Be was used, significant redistribution of the dopant occurred, which resulted in an accumulation of Be on the GaAs side of the heterointerfaces, and a maximum incorporation of Be of $\sim 5\times 10^{-17}$ cm^{-3} in the AlAs layers. Similar results were obtained for Be dopant profiles in AlGaAs/AlAs quarter-wave distributed Bragg reflectors (DBR). Be segregation and diffusion during growth resulted in a high electrical resistance in these DBR structures. The resistance was significantly reduced when the structure was doped with C.

Vertical cavity surface emitting lasers (VCSELs) are attractive devices. Their planar design and small size offer advantages in beam characteristics, scalability, fabrication, and array configurations, as opposed to their edge emitting counterparts.[1] The basic structure includes a bottom quarter wavelength distributed Bragg reflector (DBR), and a lower cladding layer, both doped *n*-type, a thin intrinsic active region, an upper cladding layer, and a top DBR, both doped *p* type. One serious problem encountered with VCSELs is an anomalously high series resistance, which is attributed to the top DBR.[2] Many attempts have been made to lower the series resistance, such as the use of graded, rather than abrupt heterointerfaces, and modulation doping.[1,3,4] These structures have resulted in about an order of magnitude lower series resistance, without sacrificing mirror reflectivity. Unfortunately, the resistance is still not low enough to achieve reasonable power efficiencies in VCSELs.

In this study, we examined the *n*- and *p*-type dopant profiles obtained in AlGaAs/AlAs DBR structures grown by molecular beam epitaxy (MBE). For *n*-type material, doped with Si, targeted dopant profiles were readily obtained. However, when Be was used as the *p*-type dopant, we observed significant redistribution during growth, resulting in an accumulation of Be at the heterointerfaces. In fact, the maximum obtainable concentration of Be in the AlAs layers was $\sim 5\times 10^{17}$ cm^{-3} at a growth temperature of 580 °C. On the other hand, when C was substituted for Be as the *p*-type dopant, the targeted dopant profiles were easily achieved with no observable redistribution. Furthermore, DBRs, doped with C, had a series resistance which was much lower than their Be-doped counterparts.

Structures were grown at 580 °C in an elemental source Intevac Gen II MBE machine, on (100) oriented, 2 in. undoped or n^+ GaAs substrates (Si doped to $\sim 1\times 10^{18}$), with substrate rotation. C doping was obtained from a heated graphite filament source as described previously.[5] Growth rate and composition calibration were achieved using reflection high energy electron diffraction intensity oscillations.[6]

Two types of structures were grown. First, Si, Be, and C dopant segregation was studied, using a simple test structure, consisting of the following four layers: 1000 Å GaAs, 1000 Å AlAs, 1000 Å GaAs, and 1000 Å AlAs, grown on undoped substrates. Both the GaAs and AlAs growth rates were 0.5 μm/h, and the entire structure was uniformly doped by maintaining a constant dopant flux during growth. Samples 1, 2, and 3 were doped with Si (3.0×10^{18} cm^{-3}), Be (2.0×10^{19} cm^{-3}), and C (2.0×10^{19} cm^{-3}), respectively. Then DBR structures, designed for a peak reflectivity at 850 nm, with 19 periods, were grown on n^+ substrates. The parameters of the DBR structures studied are listed in Table I. They were nominally uniformly doped to 5.0×10^{18} cm^{-3} with either Be or C for series resistance comparisons. The three different DBR heterointerface profiles studied, including step, linearly, and parabolically graded, are depicted in Fig. 1. Compositional grading in the linearly and parabolically graded structures was achieved by adjusting the individual thicknesses in the bilayer of a constant-period superlattice.[1]

Resonance ionization mass spectrometry (RIMS) composition versus depth profiles were obtained for the structures. Note that RIMS must be used when studying these structures, and not secondary ionization mass spectrometry, since the latter technique has severe matrix effects when analyzing for Be in changing $Al_xGa_{1-x}As$ compositions.[7] The RIMS instrument has been calibrated for $Al_xGa_{1-x}As$ with implant standards of the relevant dopant.[8] All RIMS profiles were obtained with Xe^+ sputtering. Dopant calibration was also performed on separate samples of GaAs, using Hall effect measurements.

Current-voltage (*I-V*) measurements were performed on the DBR structures using photolithographically defined 20-μm-diameter contacts and a broad area contact on the n^+-substrate side. Mesas of 4 μm depth were etched into the epitaxial layer side to avoid current spreading in the DBR region. Au/Be contacts, alloyed at 380 °C for 20 s, were used as *p*-type ohmic contacts. Broad-area Au/Ge contacts, annealed at 420 °C for 20 s, were used as *n*-type substrate contacts. The *I-V* measurements were performed with a 370 Tektronix curve tracer and a Hewlett–Packard HB 4145B parameter analyzer. The *pn* structures have rectifying *I-V* characteristics with very low leakage currents (<10 μA). In addition, reflectivity measurements were

Downloaded 30 Jun 2003 to 128.113.111.105. Redistribution subject to AIP license or copyright, see http://ojps.aip.org/aplo/aplcr.jsp

TABLE I. DBR structures studied, including electrical and optical data.

Sample	Heterointerface grading	Dopant	Differential resistance at 5 mA (Ω)	λ Center (μm)
4	step	Be	185	0.850
5	parabolic	Be	98	0.825
6	step	C	157	0.875
7	linear	C	128	0.860
8	parabolic	C	49	0.925

performed on the DBR structures using a incandescent light source (tungsten halogen) and an Anritsu 9001B optical spectrum analyzer. The reflectivity measurements were calibrated using dielectric quarter-wave mirrors with reflectivities exceeding 99.5%.

RIMS depth profiles were obtained for samples 1, 2, and 3 to study the dopant distribution obtained during growth. From the RIMS profile of sample 1, shown in Fig. 2, the Si concentration vs depth obtained is close to the targeted structure. The apparent difference in Si concentration obtained in the GaAs versus AlAs layers is due to the change in sputter rate between these two materials, which reduces the signal from the AlAs layer. The As signals are similarly affected. Notice that the ratio of the Si and As signals are constant. On the other hand, the RIMS profile of sample 2, shown in Fig. 3, indicates significant segregation of Be during growth, resulting in an accumulation of dopant on the GaAs side of the heterointerfaces. In fact, the Be appears to have a solubility limit of about 5×10^{17} cm^{-3} in AlAs, which is quite low when compared to its limit of $>1\times10^{20}$ cm^{-3} in GaAs.[9] Alternatively, when C is used as the p-type dopant, the targeted profiles were easily achieved. This is clearly seen in the RIMS profile of sample 3, shown in Fig. 4. The apparent difference in C concentration between the GaAs and AlAs layers is due to the change in sputter rate for these materials as mentioned above. C-containing impurities present at the surface and substrate/epi-interface produce peaks at these locations.

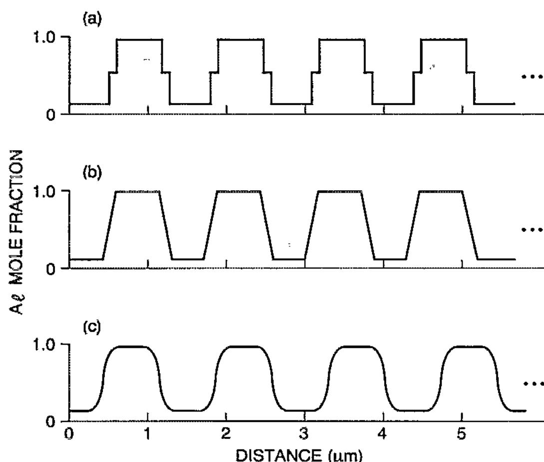

FIG. 1. Schematic representation of the three different types of graded heterointerface DBR structures studied: (a) step, (b) linear, and (c) parabolic.

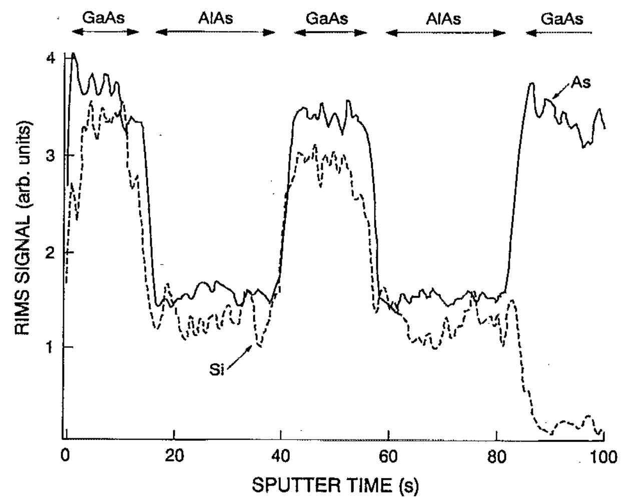

FIG. 2. RIMS depth profile of sample 1, which was uniformly doped with Si (3.0×10^{18} cm^{-3}). No redistribution of Si was detected. The difference in Si signal between the GaAs and AlAs is due to a change in sputter rate between these two materials, since the Si to As ratio is constant.

The above RIMS profiles are not surprising considering the differences in diffusivities between the three dopants studied. Although Si has a diffusion coefficient in $Al_{0.30}Ga_{0.70}As$ which is twice that in GaAs,[10] and may be even larger in AlAs, it is still low enough to avoid any observable dopant redistribution in the n-type layers at normal MBE growth temperatures (<600 °C). However, Be has a diffusivity which is at least three orders of magnitude higher than C in both AlAs and GaAs.[11] Additionally, the diffusivity of Be in $Al_{0.30}Ga_{0.70}As$ is four times larger than in GaAs,[12] and is expected to be even larger for AlAs. Both the high diffusivity, and the large difference in diffusivity of Be between GaAs and AlAs allow it to quickly diffuse out of the AlAs. Once Be reaches the GaAs layer, it slows down,which causes it to pile up at the heterointerfaces.

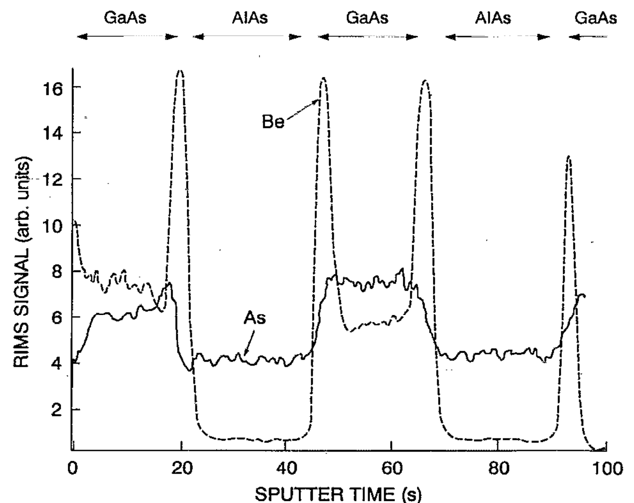

FIG. 3. RIMS depth profile of sample 2, which was uniformly doped with Be (2.0×10^{19} cm^{-3}). We observed significant redistribution of Be, resulting in an accumulation at the heterointerfaces, and a maximum concentration of $\sim5\times10^{17}$ cm^{-3} in the AlAs layers.

Downloaded 30 Jun 2003 to 128.113.111.105. Redistribution subject to AIP license or copyright, see http://ojps.aip.org/aplo/aplcr.jsp

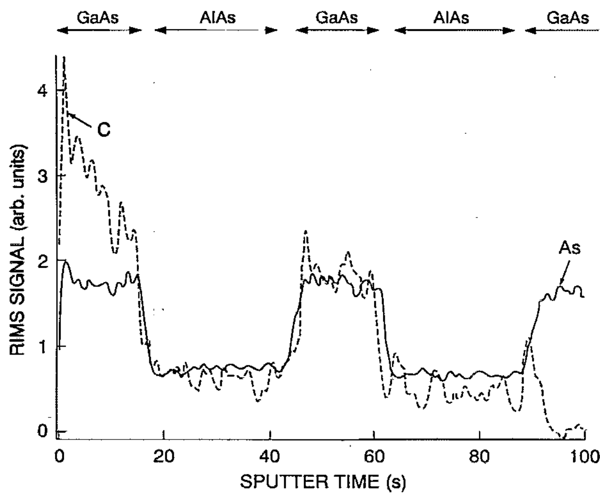

FIG. 4. RIMS depth profile of sample 3, which was uniformly doped with C (2.0×10^{19} cm^{-3}). No redistribution of C was detected. The difference in C signal between the GaAs and AlAs is due to a change in sputter rate between these two materials, since the C to As ratio is constant.

Table I lists the results obtained for the DBR structures. Reflectivity measurements indicated that they were all within 9% of the target value of 0.850 μm, with peak reflectivities greater than 97%, indicating good layer thickness control. The differential resistance of all samples was evaluated at a forward diode current of 5 mA in terms of the slope of the *I-V* characteristic. We attribute the measured resistance to the *p*-type DBR region. The differential diode resistance, the contact resistance, and the spreading resistance of the mesa structures are on the order of 2Ω and do not contribute significantly to the overall resistance ($R_{\text{contact}}=\rho_c/r^2\pi\cong1.6$ Ω; $\rho_c\cong5\times10^{-6}$ Ω cm^2; $R_{\text{spreading}}=\rho_{\text{substrate}}/4r\cong0.5$ Ω; $\rho_{\text{substrate}}\cong2\times10^{-3}$ Ω cm). The average measured resistance values are summarized in Table I. Several contacts on each sample were measured. Their resistances were within ±5 Ω of the average value. From the resistivity measurements, the C-doped samples clearly had a lower series resistance than the Be-doped samples for a given structure. The type of mirror grading also had a large impact on the resistance, where the resistivity increases in the order parabolic, linear, step graded. Previous researchers[3] have also obtained much lower resistivities for parabolically versus step-graded Be-doped DBR structures. We observe an additional reduction of a factor of 2 when the parabolically graded structure is doped with C instead of Be. To investigate this further, we performed RIMS profiles on several of the DBR structures, and observed similar results to samples 2 and 3. Significant redistribution of the Be was observed, but not the C.

The difference in resistance between the Be- and C-doped DBR structures is explained as follows. The large difference in both solubility limit and diffusivity leads to dopant segregation of the Be out of the high Al containing layers into the low Al containing layers. The resultant dopant profile has a pile up of Be at the heterointerfaces, with a much lower Be concentration in the high Al-containing (wide gap) material than the low Al-containing (narrow gap) material. The doping concentration modulation of Be-doped GaAs/AlAs multilayers seen in Fig. 3 results in a valence band-edge modulation. In order to overcome the band-edge modulation, carriers require a sufficiently large kinetic energy, which must be provided by an external bias. The effect of Be redistribution manifests itself as a high resistance of the structure.

In conclusion, we studied the Si, Be, and C dopant profiles in GaAs/AlAs structures and DBR structures grown by MBE at 580 °C. When they were doped with Si and C, the targeted dopant profiles were readily obtained. However, when the structures were doped with Be, we observed significant redistribution of the dopant, resulting in an accumulation of Be on the GaAs side of the heterointerfaces and a maximum concentration of $\sim5\times10^{17}$ cm^{-3} in the AlAs layers. Our experimental results show that the high series resistance in VCSEL structures is due to segregation of Be during growth, and a much lower solubility limit for Be in AlAs than in GaAs. These problems can be avoided by doping the structure with C.

We would like to thank A. Benvenuti and M. R. Pinto for useful discussions. We would also like to acknowledge stimulating discussions with Roger J. Malik on carbon filament doping.

[1] J. L. Jewell, J. P. Harbison, A. Scherer, Y. H. Lee, and L. T. Florez, IEEE J. Quantum Electron. **27**, 1332 (1991).
[2] L. W. Tu, E. F. Schubert, R. F. Kopf, G. J. Zydzik, M. Hong, S. N. G. Chu, and J. P. Mannaerts, Appl. Phys. Lett. **57**, 2045 (1990).
[3] E. F. Schubert, L. W. Tu, G. J. Zydzik, R. F. Kopf, A. Benvenuti, and M. R. Pinto, Appl. Phys. Lett. **60**, 466 (1992).
[4] K. Tai, L. Yang, Y. H. Wang, J. D. Wynn, and A. Y. Cho, Appl. Phys. Lett. **56**, 2496 (1990).
[5] R. J. Malik, R. N. Nottenberg, E. F. Schubert, J. F. Walker, and R. W. Ryan, Appl. Phys. Lett. **53**, 2661 (1988).
[6] R. F. Kopf, J. M. Kuo, and M. Ohring, J. Vac. Sci. Technol. B **9**, 1920 (1991).
[7] See, for example, S. W. Downey, A. B. Emerson, R. F. Kopf, and J. M. Kuo, Surface Interface Anal. **15**, 781 (1990); S. W. Downey, R. F. Kopf, E. F. Schubert, and J. M. Kuo, Appl. Opt. **29**, 4938 (1990).
[8] S. W. Downey, A. B. Emerson, and R. F. Kopf, J. Vac. Sci. Technol. B **10**, 385 (1992).
[9] E. F. Schubert, J. M. Kuo, R. F. Kopf, H. S. Luftman, L. C. Hopkins, and N. J. Sauer, J. Appl. Phys. **67**, 1969 (1990).
[10] E. F. Schubert, C. W. Tu, R. F. Kopf, J. M. Kuo, and L. M. Lunardi, Appl. Phys. Lett. **54**, 2592 (1989).
[11] C. R. Abernathy, S. J. Pearton, R. Caruso, F. Ren, and J. Kovalchick, Appl. Phys. Lett. **55**, 1750 (1989).
[12] E. F. Schubert and R. F. Kopf (unpublished).

Downloaded 30 Jun 2003 to 128.113.111.105. Redistribution subject to AIP license or copyright, see http://ojps.aip.org/aplo/aplcr.jsp